The International Journal of Advanced Manufacturing Technology (2018) 97:4081–4099
https://doi.org/10.1007/s00170-018-2241-1

ORIGINAL ARTICLE

The effect of drilling parameters, cooling technology, and fiber orientation on hole perpendicularity error in fiber metal laminates

K. Giasin[1]

Received: 26 February 2018 / Accepted: 29 May 2018 / Published online: 6 June 2018

Abstract

Conventional twist drilling is a widely used machining process for creating holes in aerospace and automobile structures. Drilling at room temperature can sometime affect the quality of machined holes due to increased thermal effects on the workpiece. Thermal effects can be a cumbersome when machining composites and fiber metal laminates due to their different thermal expansion coefficients, which may introduce additional stress in the structure. Thermal machining effects can be minimized using coolants supplied either directly or indirectly to the cutting tool-workpiece interaction zone, to remove away part of the generated heat. The use of coolants adds extra costs for handling, disposal, and environmental impact. Therefore, environmentally friendly cooling technologies are replacing conventional cooling methods to reduce costs and impact on the environment. In addition, the selection of machining parameters has great influence on the hole quality. This paper investigates the impact of drilling parameters and two modern cooling technologies namely cryogenic liquid nitrogen and minimum quantity lubrication on the hole perpendicularity error of fiber metal laminates commercially known as GLARE® (Glass Laminate Aluminum Reinforced Epoxy). It was also found that applying cryogenic liquid nitrogen or minimum quantity lubrication does not lead to an improvement in hole perpendicularity error in GLARE® laminates.

Keywords Drilling · GLARE · Perpendicularity error · Cryogenic machining, minimum quantity, lubrication · Fiber orientation

1 Introduction

Nowadays, the fuselage and wings of modern commercial aircrafts contains parts manufactured from carbon fiber-reinforced plastics (CFRP), hybrid CFRP/metal stacks (such as titanium and aluminum), and fiber metal laminates such as GLARE® (Glass Laminate Aluminum Reinforced Epoxy). The most common machining application for connecting those parts is by drilling riveted holes. The geometrical requirements for producing holes in aerospace structures are tight and carried out in one machining step with high process reliability to withstand the high loads and meet aviation safety requirements. The use of hybrid multistacked materials made up of composites and metals in aircraft structures increases the load-carrying capacity of the structure and improves their optimal performance by taking advantage of their dissimilar physical characteristics. However, this adds more difficulty in producing dimensionally accurate holes thorough the stack. Moreover, the different cutting mechanisms involved in machining hybrid stacked materials means that the cutting tool will undergo different types of wear mechanisms. Therefore, the tolerance requirements for holes in aircraft components are of primary importance. Fiber metal laminates (FMLs) are a special type of composite metal stacks in which thin metallic sheets and composite layers are bonded together using an adhesive epoxy to form a permanent structure. Airbus A380, the largest commercial aircraft in the world currently uses GLARE® FMLs in its upper fuselage making 3% of all materials used in its structure by weight. Currently, Airbus A380 uses 27 single and double curved GLARE® panels leading to 1000 kg weight savings on its upper fuselage and additional 90 kg weight reduction of the vertical edges. The thickness of GLARE® laminates can vary from less than a 1 mm and up to a 33/32 layer in highly loaded areas.

Fiber metal laminates (FMLs) are hybrid composite metal materials bonded together using adhesives. FMLs offer an attractive alternative for monolithic metal alloys in primary aircraft structures due to their superior properties such as

✉ K. Giasin
giasink@Cardiff.ac.uk

[1] Cardiff School of Engineering, Cardiff University, North/1.50, Queen’s Buildings, The Parade, Cardiff CF24 3AA, UK

fatigue and damage resistance in addition to significant weight savings [1–4]. FMLs are composed of metals usually aluminum and thermoset-based synthetic materials such as epoxy and polypropylene embedded with either glass (commercially known as GLARE®) based on R-glass or S2-glass fibers [4], Aramid (commercially known as ARALL®), or carbon (commercially known as CARALL®). Other types of metals used in FMLs include magnesium and titanium (TiGr) [3, 5, 6].

Conventional machining processes such as drilling and milling remain the most used cutting processes for composites and FMLs. The research on the machinability of FMLs have surged in the past few decades with a focus on conventional machining processes such as drilling and milling [3, 7–27] and non-conventional processes such as laser drilling and abrasive water jet cutting [15, 28–30]. The utilization of FMLs into aeronautical applications imposes many challenges for manufacturing parts with precise geometry and quality. FMLs such as GLARE® are produced in large panels of several meters in dimension. Conventional machining processes are applied to such panels to prepare them for assembly into larger structures. Machining processes are usually applied after the forming of the laminate due to limited formability of the laminate [3, 19]. Previous literature on hole making in FMLs looked into the impact of cutting parameters (spindle speed and feed rate), cutting tool size and geometry, workpiece thickness (hole depth), ply orientation, and the presence or absence of coolants on cutting forces and a variety of hole quality parameters [3, 7–27]. The studies looked into the effect of tool type, size, and coating on the hole quality [13, 31]. The finding suggested that the performance of carbide tools is better than HSS and uncoated tools due to the abrasive nature of composite layers in FMLs [3, 31]. It was also reported that two flute twist drills gave less delamination and burr formations compared to three-flute and four- and eight-facet drills [13]. The use of coolants during drilling of GLARE® was found to reduce burr formations, enhance borehole surface finish, and lower the workpiece temperature [8, 9]. The laminate thickness and fiber orientation of composite layers were found to influence a number of hole quality parameters and cutting forces [8, 9, 12, 14]. Previous studies on drilling FMLs also evaluated the hole surface roughness and circularity error for different grades and thicknesses [7, 9, 10]. However, none of the previous literature on machining FMLs reported on hole perpendicularity error. Perpendicularity error can be defined in degrees as the angle of the hole axis relative to the flat surface of the part, ideally to be perpendicular or 90° from a datum surface or line. Axis perpendicularity error is one of the more common forms of axes call outs which is used for positive and negative features (i.e., pins and holes) [32]. Perpendicularity error is an important parameter in bolted structural joints [33]. Holes which are not drilled exactly parallel to the surface of the joint reduce the contact area between the outer edges of the nut and the bolt heads with the workpiece surface causing significant stress concentrations. Indeed, 80% of fatigue cracks in aircraft body are due to poor connecting holes [34], while the fatigue fracture of fastened holes account for 50–90% of fractures in aging planes [35]. Greater perpendicularity error increases the radius of contact and causes the nut to dig into the joint which increases the torque loss, affecting the friction forces and therefore torque preload relationship [33]. Hole perpendicularity error is also important in micromachining applications, and the manufacturing of printed circuit boards requires drilling numerous numbers of high precision microholes with minimal perpendicularity error to ease the installation of microelectrical components on the circuit board [36].

Previous studies investigated the effect of cutting parameters, tool coating, tool geometry, and coolants on hole perpendicularity error for a variety of metallic materials such as steel, aluminum, and titanium alloys [37–46] and composite materials [36, 47]. The studies found that three most significant variables on hole perpendicularity error were cutting speed, feed rate, and depth of cut [40–42, 48–50]. Other studies reported that the application of machining coolants did not have an influence on the hole dimensional and positional accuracy such as its perpendicularity error and cylindricity expect for certain cases, which was mainly attributed to the size and type of cutting tool used [40]. Sheth et al. [41, 48, 49] found that the cutting speed, feed rate, and depth of cut had an impact on hole perpendicularity error when machining wrought cast steel. They also found that perpendicularity error was minimum when drilling at higher spindle speeds, lower feed rates, and lower depths of cut. The range of hole perpendicularity error can vary depending on the type of cutting process and workpiece material as depicted in Table 1. As it can be concluded from the literature, up to the knowledge of the authors, there were no studies which have previously looked into the impact of applying coolants during the machining of FMLs except in two of our previous work on drilling GLARE [8, 9]. The current study aims to fill the gap in this field and complement on our previous work, by conducting an experiment to examine the impact of cutting parameters (spindle speed, feed rate), depth of cut, and fiber orientation on hole perpendicularity error in two grades of GLARE® laminates under dry, cryogenic, and minimum quantity lubrication.

2 Materials and methods

2.1 Workpiece details and setup

Four GLARE® samples—each having dimensions of 200 mm × 150 mm—were utilized in this study: GLARE®

Table 1 Range of hole perpendicularity error for conventional and non-conventional drilling processes

Machining process	Workpiece material	Perpendicularity error range (mm)	Reference
Electrochemical drilling	Inconel 625	0.0520–0.430	[50]
Abrasive water jet machining	Inconel 617	0.0246–0.1129	[44]
Electrical discharge machining	Si3N4–TiN composite	0.038–0.598	[51]
Electrical discharge machining	MoSi2-SiC composites	0.043–0.479	[52]
Drilling	Medium carbon steel	0.0061–0.0259	[53]
Drilling	Carbon steel	0.036–0.151	[41]
Drilling	Titanium ASTM B265 Grade 2	0.008–0.045	[42]
Drilling	Aluminum	0.03–0.13	[43]
Abrasive water jet machining	Aluminum	0.05–0.25	[46]

2B and GLARE® 3. The samples consist of multiple sheets of Al2024-T3 alloy and layers of S2 glass fiber and FM94 adhesive epoxy prepregs. The samples were cured in an autoclave for around 300 min, 120 °C temperature, and a pressure of 6 bars [54]. Each glass fiber layer consists of two plies oriented at either 90°/90° or 0°/90° with respect to aluminum rolling direction (0°). An illustration of the workpiece used in drilling trials is shown in Fig. 1. Additional mechanical and thermal properties of the laminate constituents are given in Table 2. The samples were supplied by the Fiber Metal Laminate Centre of Competence (F.M.L.C) in the Netherlands.

2.2 CNC machine setup and cutting tool details

A MORI SEIKI SV-500 CNC milling machine with a maximum spindle speed of 10,000 rpm was used to carry out the drilling tests as shown in Fig. 2a. GLARE® samples were mounted and bolted to a 20-mm-thick aluminum backup plate to limit any bending or movement of laminate during the drilling process. The cutting tools used in the current study were 6-mm TiAlN-coated carbide twist drills with total length of 66 mm, 30° helix angle, and 140°-point angle as shown in Fig. 2b.

2.3 MQL drilling trials setup

The MQL drilling tests were carried out using a portable MQL system, which consists from an oil storage tank filled with a metal machining oil commercially known as COOLUBE 2210 [8, 9, 59]. The levels of flow rate and air pressure were controlled using an air pressure and flow rate control units [8, 9, 59]. Details of the MQL system and nozzle setup inside the CNC machine are shown in Fig. 3. The MQL system is capable of supplying specific amounts of the coolant mixed with high pressure compressed air at a fixed distance at the nozzle tip to disperse it towards the cutting zone under pressures ranging from 1 to 4 bars to produce coolant flow rates between 15 and 1200 ml/h [8, 9, 59]. Three levels of flow rate and air pressure were used: 20, 40, and 60 ml/h and 1, 2, and 3 bars. The choice of those levels was based on previous studies on MQL drilling of aluminum alloys which applied flow rates in the range of 10 to 100 ml/h and in some cases up to 250 ml/h [8, 9, 59–68].

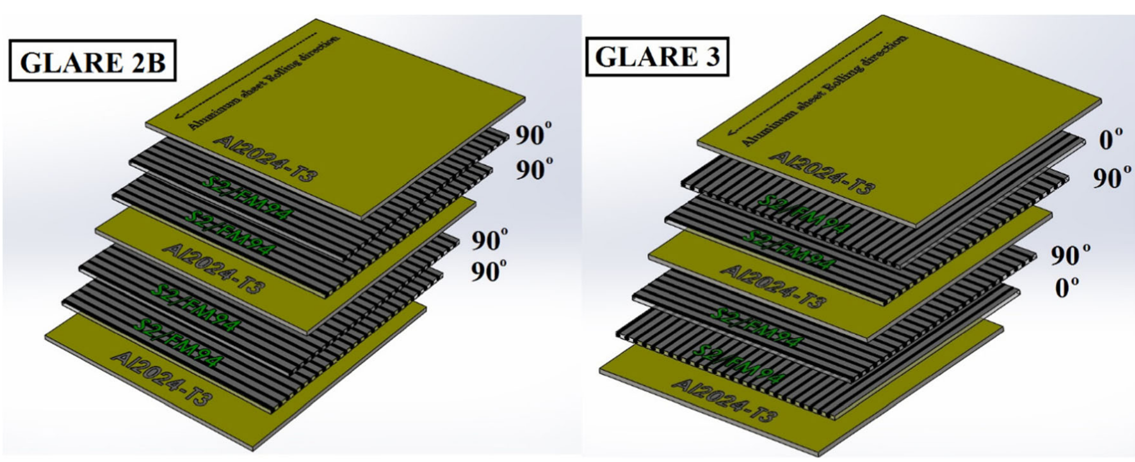

Fig. 1 Schematic representation of the GLARE® grades 2B and 3 laminates used in the drilling trials

Table 2 Mechanical properties of S2-glass fiber prepreg and Al2024-T3 [9, 11, 55–58]

Mechanical property		Unidirectional S2 glass/FM 94 epoxy prepreg $V_F = 60\%$	Al2024-T3	Units
Young's modulus (E)	L	54–55	72.2	GPa
	T	9.4–9.5	–	
Ultimate tensile strength (σ)	L	2640	455	MPa
	T	57	448	
Ultimate strain % (ε)	L	3.5–4.7	19	–
	T	0.6	–	
Shear modulus (G)	L	5.55	27.6	GPa
	T	3	–	
Poisson's ratio (ν)	L	0.33	0.33	–
	T	0.0575	–	
Density (ρ)	–	1980	2770	kg/m^3
Thermal expansion coefficient (α)	L	3.9–6.1	23.4	(1/°C) ·10–6
	T	26.2–55.2	23.4	
Thermal conductivity (K)	L	1.1–1.4	121	W/m-K
	T	0.43–0.53	–	

The symbols L and T stands for longitudinal (the rolling direction for the metal) and transverse directions respectively

2.4 Cryogenic drilling trials setup

The cryogenic coolant was delivered directly from a portable Statebourne self-pressurized liquid nitrogen dewar with a maximum capacity of 90 l and a maximum operating pressure of 3 bars [8, 9, 59]. Details of the experimental setup for cryogenic drilling trials are given in Fig. 4. The cryogenic coolant was transferred from the tank to the cutting zone through a 4-m vacuum-insulated stainless steel hose at a fixed pressure of 2 bars and a flow rate of 8 l/min at 1.5 bars [8, 9, 59].

Three levels of spindle speed and feed rate were used for dry, cryogenic, and MQL drilling test. The tests were repeated two additional times (for MQL and cryogenic) and three additional times (for dry drilling) to confirm the repeatability of the results observed and all measurements were reported as mean values of the average readings obtained from the runs. In addition, three levels of air pressures and flow rate were used for the MQL trials as shown in in Table 3.

2.5 Hole perpendicularity error measurement

The measurements were carried out using Sheffield Cordax-D8 coordinate measuring machine available at Sandvik Coromant in Sheffield, UK, as shown in Figs. 3b and 5a. The machine is equipped with a TESASTAR-m motorized indexing probe head with the kinematic joint and touch trigger probing system with angular positioning and rotation by step of 5°. The machine has a resolution (displayed) of 0.000004 and repeatability (range) of 0.00012. The samples were clamped on the CMM table as shown in Fig. 5a. The CMM records the coordinates of discrete points on the borehole surface and the CMM software calculates the desired geometric

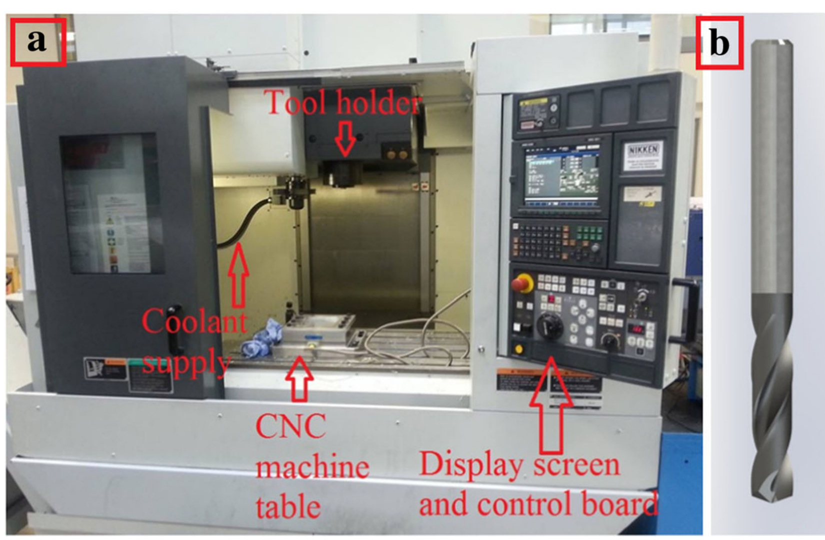

Fig. 2 **a** MORI SEIKI CNC vertical machining center. **b** OSG® HYP-HP-3D drill bit

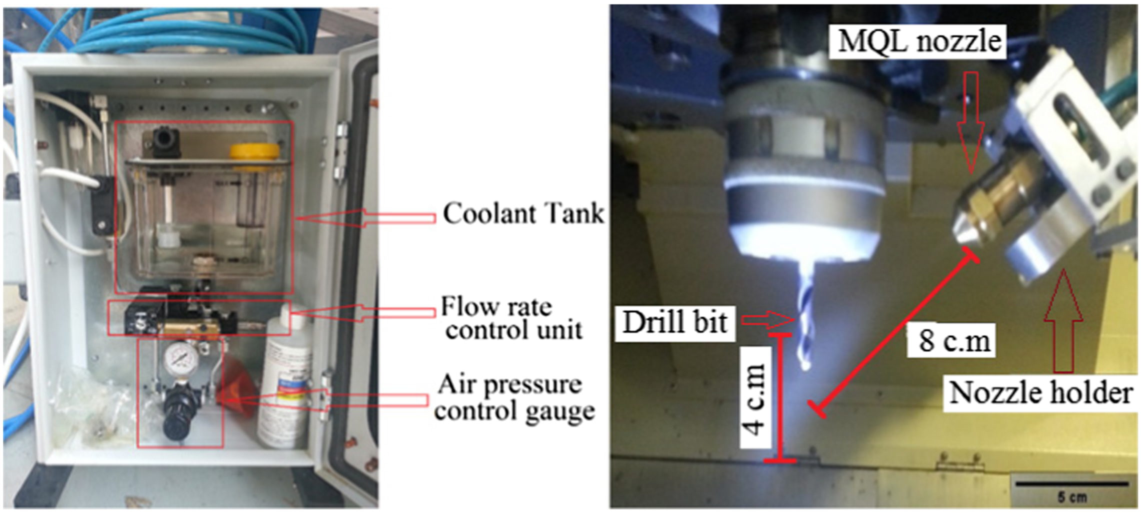

Fig. 3 Characteristics of the MQL unit and nozzle setup inside the CNC machine [8, 9]

condition based on the collected surface points coordinate data measurements as shown in Fig. 5b. To measure perpendicularity error, the workpiece level of alignment must be set by defining a reference plane. The top plane of the workpiece was taken as a reference to guarantee that the probe head will be normal to the workpiece which was mapped using several points on the top surface. The deviation of hole axis with respect to the reference plane (top plane) represents the value of hole perpendicularity error. Figure 5c shows the schematic sketch showing hole perpendicularity error in 2D view of the GLARE® laminate.

2.6 Cutting forces measurement (F_x, F_y, and F_z)

In this study, the average maximum forces in the X and Y directions acting on the hole walls developed during the drilling process were measured from the time of the initial contact of the drill with the workpiece until the completion of the drilling cycle similar to previous studies [9, 12, 59]. The cutting forces were measured using a piezoelectric 3-component dynamometer. KISTLER 9255B and 9255C dynamometers were used to measure the planar orthogonal components (F_x and F_y) of a force during the machining process [9, 12, 59]. The dynamometers are identical in dimensions but differ in their measuring range. The dynamometer has four three-component force sensors which are sensitive to pressure in the X, Y, and Z directions and can measure the cutting forces and torques in three dimensions. The dynamometer sensors are ground-insulated, are rust proof, and protected against penetration of coolants [9, 12, 59]. The dynamometer was connected to a 5070A multichannel charge amplifier for multicomponent force measurement and a KISTLER 5697A

Fig. 4 Experimental setup for cryogenic drilling trials [8]

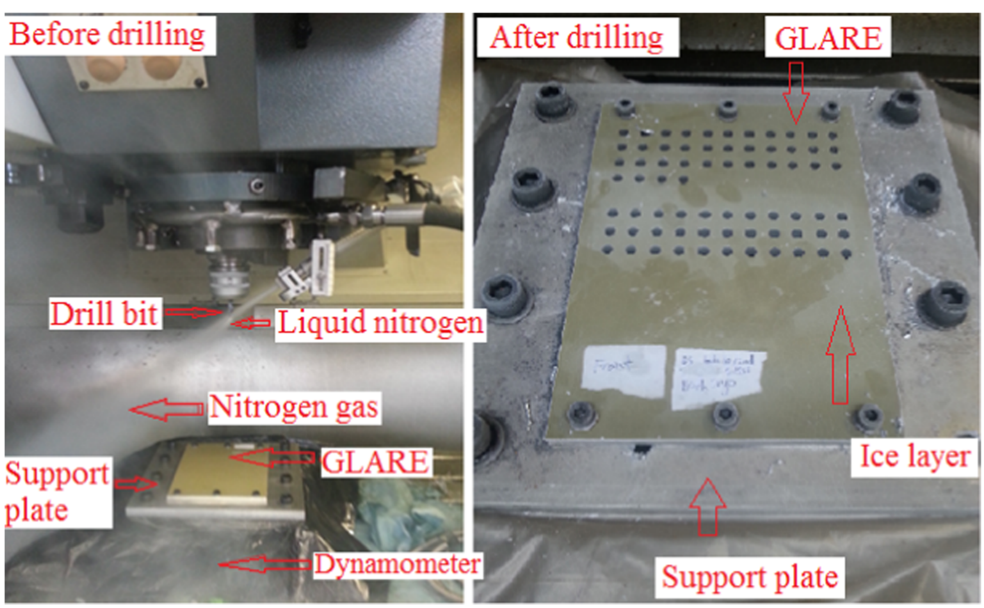

Table 3 Cutting parameters and their levels for MQL, cryogenic, and dry machining parameters and their levels [8, 9, 59]

	MQL drilling trials			Cryogenic and dry drilling trials		
Machining parameters	Low	Medium	High	Level 1	Level 2	Level 3
Feed rate (f) (mm/min)	300	600	900	300	600	900
Spindle speed (n) (rpm)	3000	6000	9000	3000	6000	9000
Flow rate (ml/h)	20	40	60	–	–	–
Air pressure (bar)	1	2	3	–	–	–

data acquisition system as shown in Figs. 1b and 6a. The charge amplifier is controlled by a data acquisition box (DAQ) which holds the dongle (HASP) key license [9, 12, 59]. A six-component force and moment measurement were used. The dynamometer is mounted with four M18 bolts from its sides on the table of the CNC machine. The measurement signals from the sensors which represent the cutting forces acting on the dynamometers are converted into an electrical voltage in the individual channels. Therefore, the measured data from the dynamometer require signal conditioning using a multichannel charge amplifier to build a complete measuring system which is controlled via DynoWare software V 2.6.5. The DAQ box and the charge amplifier are connected via an RS-232 interface. The DAQ box is connected to a PC using USB 2.0 interface. The PC is running on Windows 8 and a DynoWare software is installed. The software is used for measuring forces with dynamometers and for data post-processing. The complete setup of cutting force measurement is

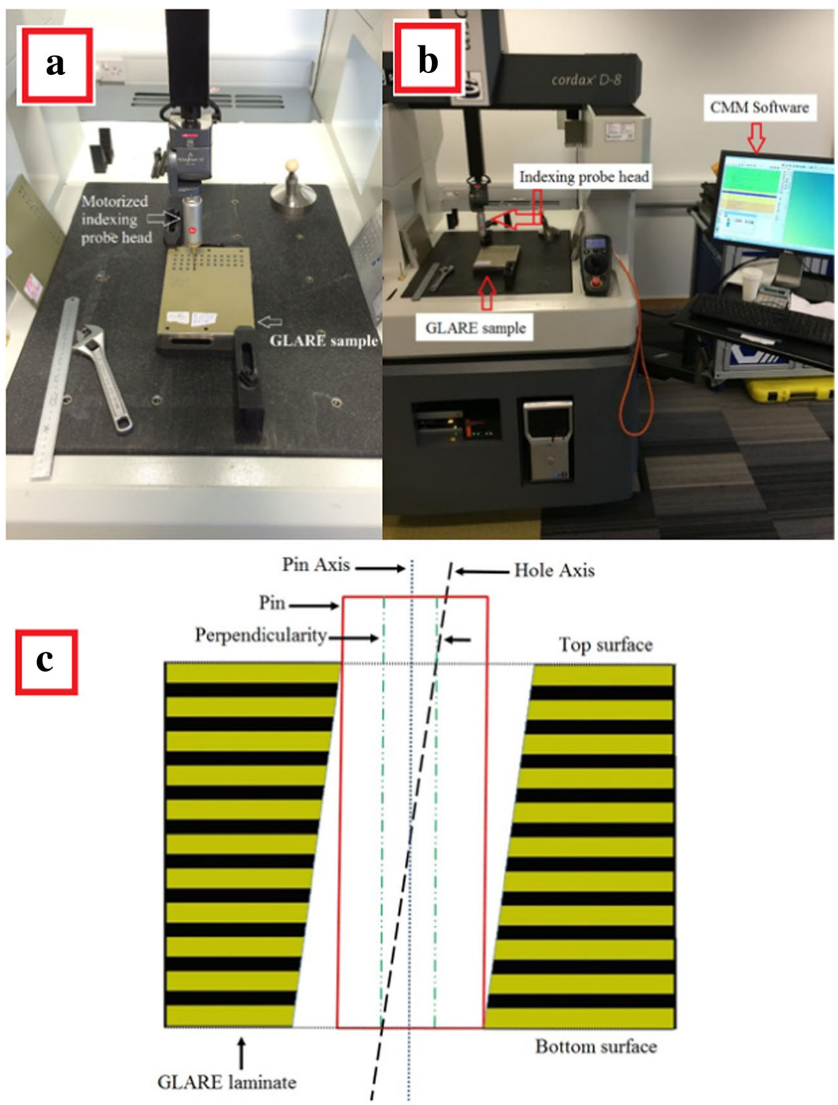

Fig. 5 **a** Details of the hole perpendicularity error measurement setup. **b** Sheffield Kordax D-8 CMM machine available at Sandvik Coromant. **c** Schematic sketch of the hole perpendicularity error in GLARE® laminates

shown in Fig. 6a, b. The cutting forces (Fx, Fy, and Fz reported in a previous study) are directly calculated during the drilling process as shown Fig. 6c, d. The sampling frequency was set to 8000 Hz and measuring time was set to 20 s for each hole drilling to allows sufficient time for recording the complete drilling process [9, 12, 59]. The cutting forces in the X, Y and Z directions are calculated as shown in the following equations. Fx12, Fx34, Fy14, Fy23, Fz1, Fz2, Fz3 and Fz4 are the acquired force components from the four piezoelectricsensors [59].

$$X\text{−force component} = F\text{x} = F\text{x}12 + F\text{x}34$$

$$Y\text{−force component} = F\text{y} = F\text{y}14 + F\text{y}23$$

$$Z\text{−force component} = F\text{z} = F\text{z}1 + F\text{z}2 + F\text{z}3 + F\text{z}4$$

3 Results and discussion

The complete set of data for hole perpendicularity error for dry, cryogenic, and MQL conditions are provided in Tables 4, 5, 6, and 7. Figure 7a shows the results of hole perpendicularity error for different hole depths in GLARE® 2B laminates under different spindle speeds and feed rates. Figure 7b–d show the corresponding cutting forces in the X, Y, and Z directions acting on the hole. The results plotted here are the average values of the four repetitions provided previously in Table 4. It should also be noted that the analysis discussion is based on average values of the results due to the large variation between each run within each drilling condition.

The results indicate that both cutting parameters and depth of cut had an impact on hole perpendicularity error. Previous reports on hole perpendicularity error in aeronautical structures shows that a face to bore perpendicularity error of 0.01 mm or less is desired [69]. Hole perpendicularity error ranged between 0.004 to 0.012 mm which is within the range of previously reported hole perpendicularity error values when drilling aluminum alloys [43]. The maximum hole perpendicularity error value occurred at a feed rate of $f = 900$ mm/min and was minimum at a feed rate of $f = 300$ mm/min. Similar trends were observed by previous researchers when drilling aluminum and titanium alloys [42, 43]. Generally, it was observed that hole perpendicularity error increased with the increase of the feed rate for all depths of cuts which is mainly due to the increase in the feed force as it can be seen from Fig. 7b due to the increases the cutting tool-workpiece vibrations and uncut chip thickness. The increase in vertical force can make the drilling process susceptible to vibrations due to increased compression by the cutting tool on the workpiece, which leads to increased perpendicularity errors. This results of cutting forces generated on the hole walls in the X and Y directions indicated that the acting X and Y forces are likely to be higher in thinner laminates when drilling at spindle speeds of 6000 and 9000 rpm as it can be seen in Fig. 7c, d. However, it was also observed that the acting X and Y forces are likely to be higher in thicker laminates when drilling at spindle speeds of 3000 rpm as it can be seen in Fig. 7c, d.

The dimensional stability of a material depends on its thermal expansion and coefficient of thermal expansion of its constituents, and their impact becomes critical at elevated temperatures such as those generated during machining processes. The thermal expansion coefficient and thermal conductivity of Al2024-T3 sheets is 23.4 × 10^{-6} 1/°C and 121 W/ m-K, respectively. For the S2 glass/FM94 epoxy prepreg are 3.9-6.1 ×10^{-6} 1/°C and 26.2-55.2 × 10^{-6} 1/°C, and 1.1–1.4 W/m-K and 0.43–0.53 W/m-K in the longitudinal and transverse fiber directions, respectively [55]. This means that the metal and composite layers in GLARE® will react differently due to the change in workpiece temperature. The shrinkage and thermal expansion/contraction in glass fiber layers are greater than that in aluminum sheets, which cause variations in the holes size. In addition, chip formation modes in glass fiber layers in the form of fiber pull-outs is observed which leaves small cavities in the laminate, while interlayer burrs are formed on aluminum sheets which cause variations in the hole geometry across different layers that directly influence hole perpendicularity. It was observed that hole perpendicularity error is likely to be higher in thinner laminates under same cutting parameters, which could be due to the increased out of plane bending of the laminate which was observed in a previous study [59]. The increased out of plane bending in thin GLARE® laminates indicate that bending deformations could adversely increase hole perpendicularity error. Generally, it was observed that increasing the spindle speed tended to decrease perpendicularity error which was also observed in a previous study [41], which is mainly due to reduced chip thickness. However, its influence was less significant than the feed rate and varied depending on the level of the feed rate and hole depth. For example, increasing the spindle speed from $n = 3000$ rpm to $n = 6000$ rpm when drilling GLARE® 2B 11/10 at a fixed feed rate tended to increase hole perpendicularity error, which could be due to the rise in cutting temperatures with depth as reported in a previous study on drilling GLARE® 2B 11/10 [11]. In addition, drilling GLARE® 2B 8/7 and GLARE® 2B 4/3 at similar parameters tended to reduce hole perpendicularity error. This could be due to the increased bending in thinner GLARE® laminates due to the absence of support plate beneath.

Figure 8a shows the influence of fiber orientation in the laminate on hole perpendicularity error for different cutting parameters. The results indicate that hole perpendicularity error is likely to be higher in GLARE® laminates with fibers oriented at same direction (i.e., 90°/90°) compared to cross-plied GLARE® laminates (i.e., 0°/90°). This might be related to the machining temperature effect on the thermal expansion

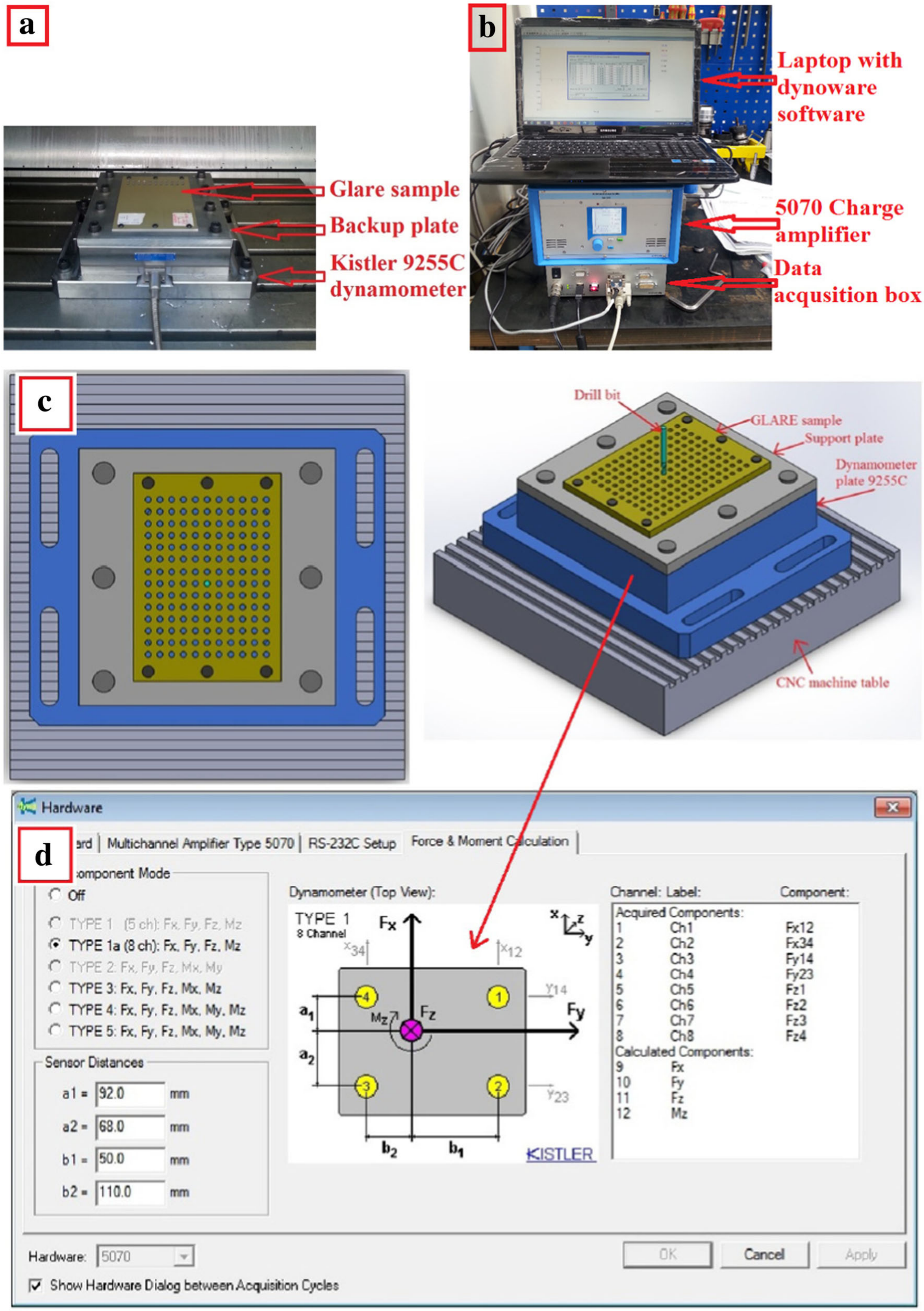

Fig. 6 **a** Workpiece and dynamometer assembly inside CNC machine. **b** Dynamometer force measurement setup [9, 12, 59]. **c** 3D views of the setup of the dynamometer, the support plate, and the workpiece inside the CNC machine [59]. **d** DynoWare software torque calculations setup and data input [59]

Table 4 Cutting parameters and results of hole perpendicularity error for holes drilled in GLARE® 2B and GLARE® 3 laminates

Cutting parameters		GLARE® 2B 11/10					GLARE® 2B 8/7					GLARE® 2B 4/3					GLARE® 3 8/7				
Spindle speed (rpm)	Feed rate (mm/min)	Test No.				Avg.	Test No.				Avg.	Test No.				Avg.	Test No.				Avg.
		1	2	3	4		1	2	3	4		1	2	3	4		1	2	3	4	
3000	300	0.003	0.011	0.005	0.001	0.005	0.005	0.012	0.004	0.010	0.008	0.005	0.004	0.016	0.005	0.008	0.004	0.004	0.003	0.003	0.004
	600	0.012	0.005	0.008	0.003	0.007	0.009	0.010	0.003	0.013	0.009	0.001	0.005	0.019	0.008	0.008	0.008	0.006	0.006	0.004	0.006
	900	0.007	0.007	0.003	0.008	0.006	0.009	0.008	0.004	0.019	0.010	0.004	0.012	0.023	0.008	0.012	0.007	0.008	0.005	0.013	0.008
6000	300	0.002	0.010	0.003	0.009	0.006	0.008	0.007	0.002	0.011	0.007	0.006	0.015	0.005	0.008	0.009	0.001	0.008	0.002	0.011	0.006
	600	0.005	0.005	0.010	0.005	0.006	0.006	0.005	0.004	0.010	0.006	0.004	0.015	0.010	0.004	0.008	0.002	0.014	0.004	0.006	0.006
	900	0.014	0.011	0.013	0.011	0.012	0.009	0.011	0.007	0.005	0.008	0.005	0.021	0.007	0.013	0.011	0.007	0.010	0.005	0.000	0.006
9000	300	0.007	0.003	0.003	0.003	0.004	0.004	0.004	0.009	0.001	0.004	0.002	0.014	0.009	0.003	0.007	0.008	0.003	0.007	0.013	0.008
	600	0.008	0.014	0.009	0.005	0.009	0.005	0.004	0.008	0.007	0.006	0.004	0.003	0.018	0.003	0.007	0.011	0.003	0.007	0.001	0.011
	900	0.007	0.007	0.006	0.005	0.006	0.004	0.005	0.005	0.005	0.005	0.005	0.007	0.012	0.001	0.006	0.010	0.005	0.006	0.003	0.010

Table 5 Cutting parameters and results of cutting forces F_x and F_y for holes drilled in GLARE® 2B and GLARE® 3 laminates

	Cutting parameters		GLARE® 2B11/10					GLARE® 2B 8/7					GLARE® 3 8/7					GLARE® 2B 4/3				
			Test No.				Avg.	Test No.				Avg.	Test No.				Avg.	Test No.				Avg.
	Spindle speed (rpm)	Feed rate (mm/min)	1	2	3	4		1	2	3	4		1	2	3	4		1	2	3	4	
X force component	3000	300	22	25.17	22.35	21.37	22.72	18.98	16.41	17.24	19.19	17.96	15.36	14.67	12.74	14.27	14.26	22.42	23.04	21.99	23.25	22.68
		600	25.76	27.48	25.4	26.6	26.31	16.1	13.05	18.82	19.07	16.76	16.73	16	18.08	17.91	17.18	21.94	23.81	21.27	22.14	22.29
		900	26.37	30.23	29.18	27.39	28.29	20.02	18.3	22.7	23.85	21.22	17.59	17.23	17.4	16.92	17.29	24.19	26.71	26.04	25.16	25.53
	6000	300	24.4	23.63	22.23	24.16	23.61	17.32	15.72	15.91	21.03	17.5	15.94	13.27	16.62	16.64	15.62	27.28	28.29	26.71	27.21	27.37
		600	22.2	23.81	25.48	24.63	24.03	18.57	15.02	15.04	16.55	16.3	12.12	11.61	11.329	12.08	11.78	28.4	28.65	27.75	25.58	27.6
		900	26.85	27.46	27.98	26.71	27.25	18.77	25.07	17.82	18.66	20.08	17.9	17.56	16.16	18.4	17.51	34	33.37	34.21	33.46	33.76
	9000	300	21.3	24.81	24.63	22.89	23.41	26.33	26.13	24.08	26.18	25.68	13.91	14.16	15.34	16.88	15.07	23.71	27.67	26.38	25.22	25.75
		600	22.17	24.84	25.48	23.74	24.06	19.92	18.84	18.53	19.85	19.29	16.85	16.53	15.55	16.22	16.29	24.85	25.85	27.05	26.08	25.96
		900	21.6	23.08	23.43	23.7	22.95	15.05	16.28	21.91	16.47	17.43	14.85	14.32	15.86	16.88	15.48	25.85	26.11	25.57	26.66	26.05
Y force component	3000	300	23	25.33	23.2	22.74	23.57	18.03	19.54	19.88	21.24	19.67	15.26	14.24	14.57	15.78	14.96	21.4	22.32	19.24	21.14	21.03
		600	24.47	25.47	25.15	24.4	24.87	20.24	18.93	19.62	19.08	19.47	20.77	17.88	18.94	20.69	19.57	22.54	23.96	21.42	21.5	22.36
		900	27.56	26.47	29.38	29.6	28.25	23.57	25.58	23.83	23.01	24	17.14	17.73	18.47	19.53	18.22	25.71	22.9	25.77	22.45	24.21
	6000	300	22.66	23.31	24.01	21.92	22.98	15.88	13.16	14.43	19.06	15.63	13.46	14.29	15.1	14.46	14.33	24.5	23.96	22.92	23.16	23.64
		600	19.85	23.1	22.63	20.58	21.54	16.36	14.22	14.46	14.13	14.79	16.61	18.42	17.89	18.9	17.96	22.8	23.15	25.16	24.47	23.9
		900	22.18	25.99	22.94	20.23	22.84	20.35	18.63	17.51	18.13	18.66	15.73	14.86	13.99	14.89	14.87	24.3	29.01	25.21	26.1	26.16
	9000	300	19.96	19.19	17.85	18.26	18.82	21	19.21	25.95	28.21	23.59	13.58	13.13	13.78	15.43	13.98	22.49	25.58	25.8	24.25	24.53
		600	19.23	19.37	18.1	21.43	19.53	18.06	18.9	19.29	20.01	19.07	11.18	13.27	11.05	12.03	11.88	22.29	22.53	20.34	22.14	21.83
		900	22.73	21.51	24.71	21.51	22.62	18.45	18.93	23.53	22.22	20.78	14.01	15.9	15.63	16.38	15.48	31.41	32.72	28.37	29.18	30.42

Table 6 Cutting parameters and results of hole perpendicularity error and maximum cutting forces F_x and F_y for holes drilled in GLARE® 2B laminates under cryogenic cooling condition

Cutting parameters		Perpendicularity error (mm)				Maximum force in X direction (N)				Maximum force in Y direction (N)			
		Test No.			Avg.	Test No.			Avg.	Test No.			Avg.
Spindle speed (rpm)	Feed rate (mm/min)	1	2	3		1	2	3		1	2	3	
3000	300	0.011	0.016	0.009	0.012	20.16	22.64	21.61	21.47	25.82	24.27	22.56	24.22
	600	0.013	0.011	0.011	0.012	21.13	25.77	26.93	24.61	32.43	30.47	31.51	31.47
	900	0.018	0.014	0.019	0.017	30.90	29.81	31.37	30.69	36.00	31.77	32.52	33.43
6000	300	0.021	0.019	0.018	0.019	23.35	27.99	27.07	26.14	25.13	24.90	28.91	26.31
	600	0.023	0.03	0.025	0.026	24.53	25.75	23.07	24.45	30.78	27.31	28.09	28.73
	900	0.024	0.022	0.024	0.023	28.04	31.75	28.25	29.35	35.21	29.41	30.38	31.67
9000	300	0.026	0.027	0.032	0.028	24.12	29.35	25.32	26.26	27.78	30.55	28.32	28.88
	600	0.02	0.022	0.031	0.024	34.94	35.83	30.83	33.87	27.89	32.07	28.63	29.53
	900	0.018	0.022	0.032	0.024	32.79	34.87	31.67	33.11	26.08	28.62	25.02	26.57

of GLARE® constituents as reported earlier. Giasin et al. [11] previously reported that maximum workpiece temperatures at the exit side of the hole in GLARE® 2B laminates was higher than those found in GLARE® 3 for the same depth of cut. In addition, previous studies reported that the drilling temperature depends on the fiber orientation which is higher for laminates with 90° fiber orientation than with 0° due to higher failure stresses [70, 71]. The rise in workpiece temperature increases the thermal distortions in the laminate and hence influencing hole perpendicularity error.

Table 7 Cutting parameters and results of hole perpendicularity error and maximum cutting forces F_x and F_y for holes drilled in GLARE® 2B laminates under minimum quantity lubrication

Cutting parameters		Coolant parameters		Perpendicularity error (mm)				Maximum force in X direction (N)				Maximum force in Y direction (N)			
				Test No.			Average	Test No.			Average	Test No.			Average
Spindle speed (rpm)	Feed rate (mm/min)	Flow rate (mm)	Air pressure (bar)	1	2	3		1	2	3		1	2	3	
3000	300	20	1	0.013	0.006	0.005	0.008	24.05	24.91	23.37	24.11	21.10	19.73	20.54	20.46
9000			1	0.006	0.005	0.006	0.006	28.69	27.12	27.25	27.69	26.96	24.47	26.84	26.09
3000	900		1	0.019	0.013	0.014	0.015	26.80	30.14	28.02	28.32	24.27	28.99	25.46	26.24
9000			1	0.009	0.009	0.007	0.008	24.99	24.13	23.16	24.09	24.85	25.49	23.17	24.50
3000	300	60	1	0.002	0.006	0.003	0.004	21.31	22.14	23.27	22.24	20.06	18.70	21.50	20.09
9000			1	0.004	0.005	0.004	0.004	24.61	25.58	27.09	25.76	23.31	26.32	26.04	25.22
3000	900		1	0.011	0.01	0.004	0.008	22.31	25.43	23.61	23.78	21.36	23.95	22.98	22.76
9000			1	0.008	0.008	0.004	0.007	26.27	27.42	23.56	25.75	26.31	25.91	22.09	24.77
3000	300	20	3	0.007	0.004	0.01	0.007	22.33	23.28	22.44	22.68	20.73	18.15	21.05	19.98
9000			3	0.006	0.002	0.007	0.005	25.46	24.39	25.91	25.25	24.63	24.86	27.04	25.51
3000	900		3	0.016	0.011	0.011	0.013	27.20	27.22	24.30	26.24	22.10	26.70	24.77	24.52
9000			3	0.012	0.004	0.007	0.007	24.90	25.91	22.53	24.45	24.30	22.91	24.26	23.82
3000	300	60	3	0.013	0.007	0.006	0.009	22.67	22.73	22.05	22.48	19.04	15.10	20.75	18.30
9000			3	0.003	0.004	0.007	0.005	26.15	26.90	27.36	26.80	25.87	25.71	26.13	25.90
3000	900		3	0.003	0.007	0.001	0.004	27.37	24.66	26.59	26.21	25.78	26.78	26.41	26.32
9000			3	0.007	0.007	0.008	0.007	26.43	26.81	26.31	26.52	24.80	24.03	24.77	24.53
6000	600	40	2	0.002	0.006	0.004	0.004	16.81	15.08	16.40	16.10	19.58	18.83	19.67	19.36
6000			2	0.007	0.003	0.002	0.004	15.10	14.42	16.88	15.47	21.05	18.51	18.79	19.45

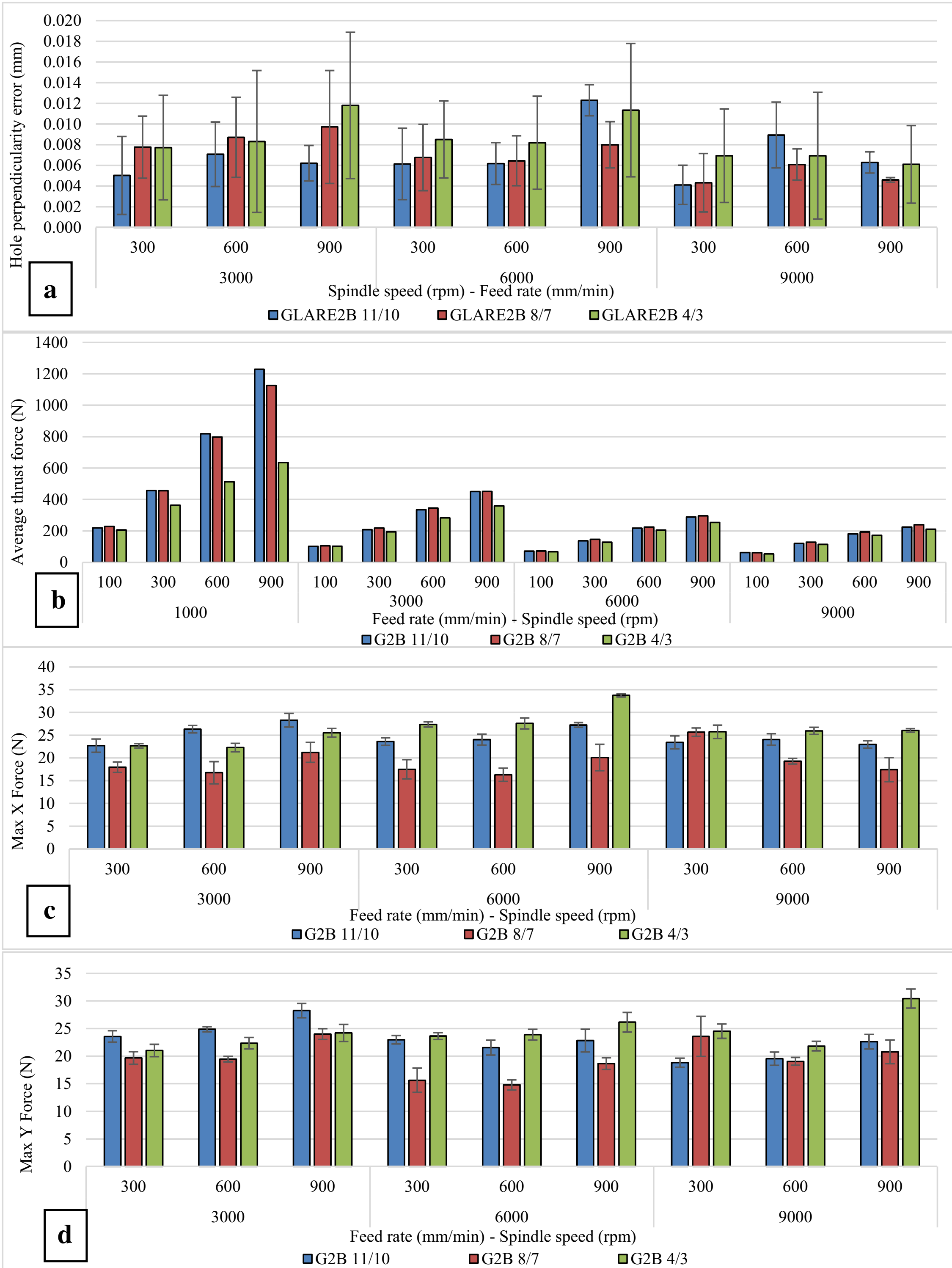

Fig. 7 The effect of workpiece thickness on **a** hole perpendicularity error, **b** average thrust force (F_z) [9, 59], **c** average maximum force in X direction (F_x), and **d** average maximum force in Y direction (F_y)

It was also observed that the cutting forces in the X and Y directions were greater in GLARE® 2B than in GLARE® 3 laminates for same cutting parameters as it can be seen from Fig. 8c, d. Generally, hole perpendicularity error in GLARE® 3 increased with the increase of the feed rate and decreased with the increase of the spindle speed as it can be seen from Fig. 8b. In addition, drilling at spindle speed/feed rate ratio of 0.1 (mm/rev) tended to decrease perpendicularity error in GLARE® 2B laminates while it tended to increase in GLARE® 3 laminates. Previous study on drilling GLARE®

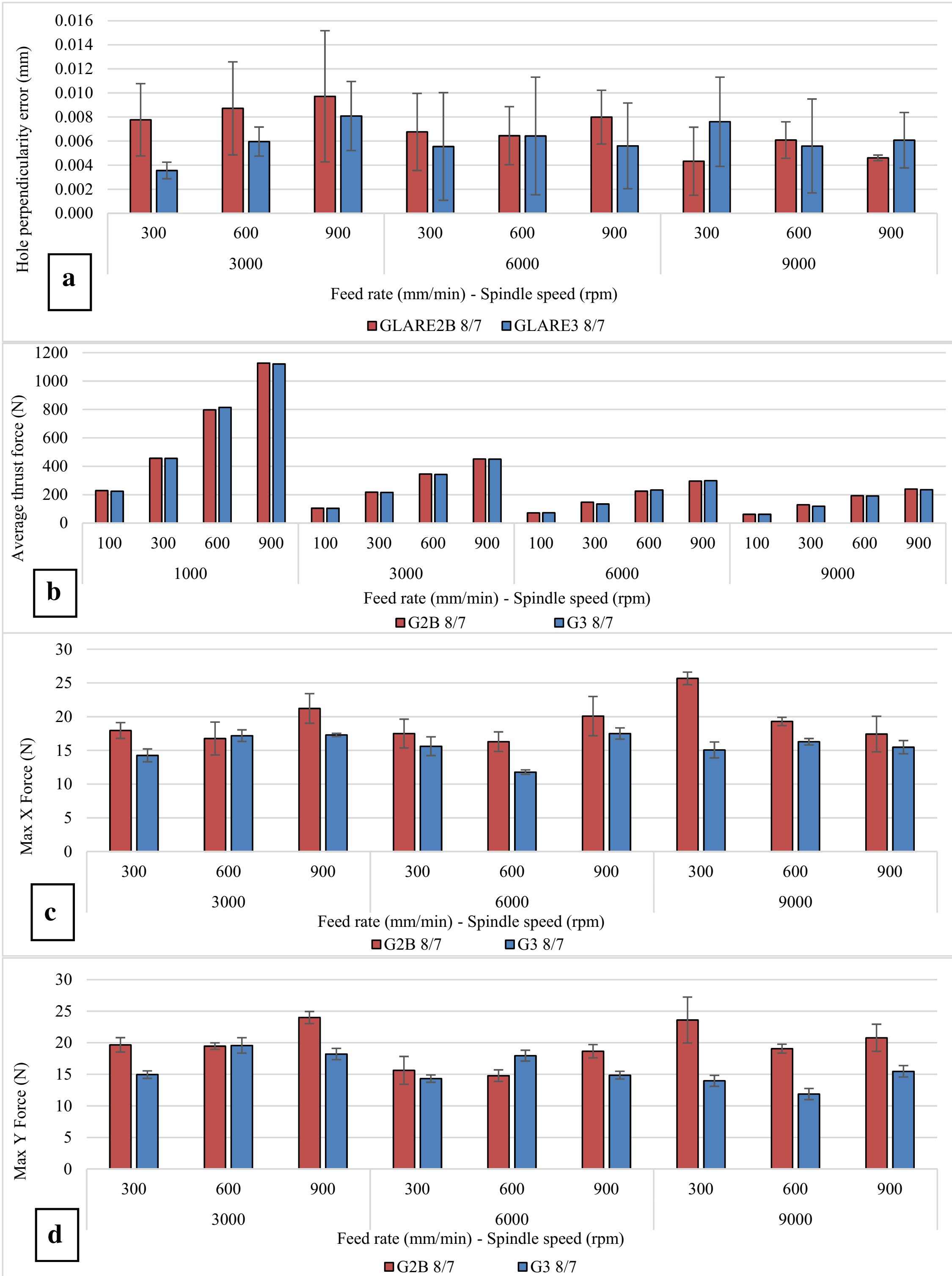

Fig. 8 The effect of fiber orientation in GLARE® laminates on **a** hole perpendicularity error, **b** average thrust force (F_z) [9, 59], **c** average maximum force in X direction (F_x), and **d** average maximum force in Y direction (F_y)

laminates reported that the damage in GLARE 3 8/7 was more severe than in GLARE 2B 8/7 [7]. The fiber orientation in the glass fiber layers dictates the severity of the damage in the laminate [7, 72]. The impact of the feed rate on GLARE® 3 is greater than that on GLARE® 2B laminates due to weaker interlaminar interface in laminates with cross ply orientations making them mechanically weaker than unidirectional ply laminates which becomes more significant at higher feed rates and spindle speeds [73]. In addition, despite having higher X and Y forces acting on the hole in GLARE 2B laminates at the highest spindle speed of $n = 9000$ mm/min, higher perpendicularity errors were observed in GLARE® 3, and this could be due to the mismatch in coefficient of thermal expansion (C.T.E.) between cross ply laminates in GLARE® 3 which affects the dimensional stability of the hole especially at higher spindle speeds [74].

By analyzing the data in Fig. 9, it can be observed that the average hole perpendicularity error increased with the increase of the feed rate due to the increase in the uncut chip thickness, which deteriorated the borehole walls. It also increased with the increase of the spindle speed due to the increase in machining temperatures, which could soften the epoxy matrix in the laminate. The increase in hole perpendicularity error with the increase of the spindle speed was greater than that due to the increase of the feed rate. Higher feed rates increases the uncut chip thickness and causes damage to the fiber layers in the form of matrix degradation and fiber pull outs in the laminate [75], while higher spindle speeds increases the rubbing of the cutting tool against the workpiece constituents causing higher thermal distortions in the hole [11]. The maximum hole perpendicularity was measured at $n = 9000$ rpm, $f = 300$ mm/min. The minimum hole perpendicularity was measured at $n = 3000$ rpm, $f = 600$ mm/min. It was also observed that hole perpendicularity error values at $n = 9000$ rpm are like those obtained at $n = 6000$ rpm which indicates that the impact of the cryogenic coolant becomes more significant at higher spindles speeds where workpiece/cutting tool temperatures are expected to be higher. When drilling at room temperature, the increase in spindle speed resulted in reduction of cutting forces due to the softening of the epoxy matrix in the GLARE® laminate [9, 11, 12, 76, 77] as shown earlier. However, the use of cryogenic coolant prevents significant temperature rise in the workpiece. Therefore, reducing the thermal softening that is expected to occur in the epoxy matrix of the laminate [77]. This was evident by the higher thrust force observed while drilling GLARE® laminates using cryogenic coolant compared to dry drilling even at higher spindle speeds [9] as it will be shown later in Fig. 11b. The adverse effect of applying cryogenic coolant can be linked to the increased hardness of the workpiece material by up to 10% under cryogenic cooling conditions due to extreme low temperatures of liquid nitrogen (− 187 °C) [9].

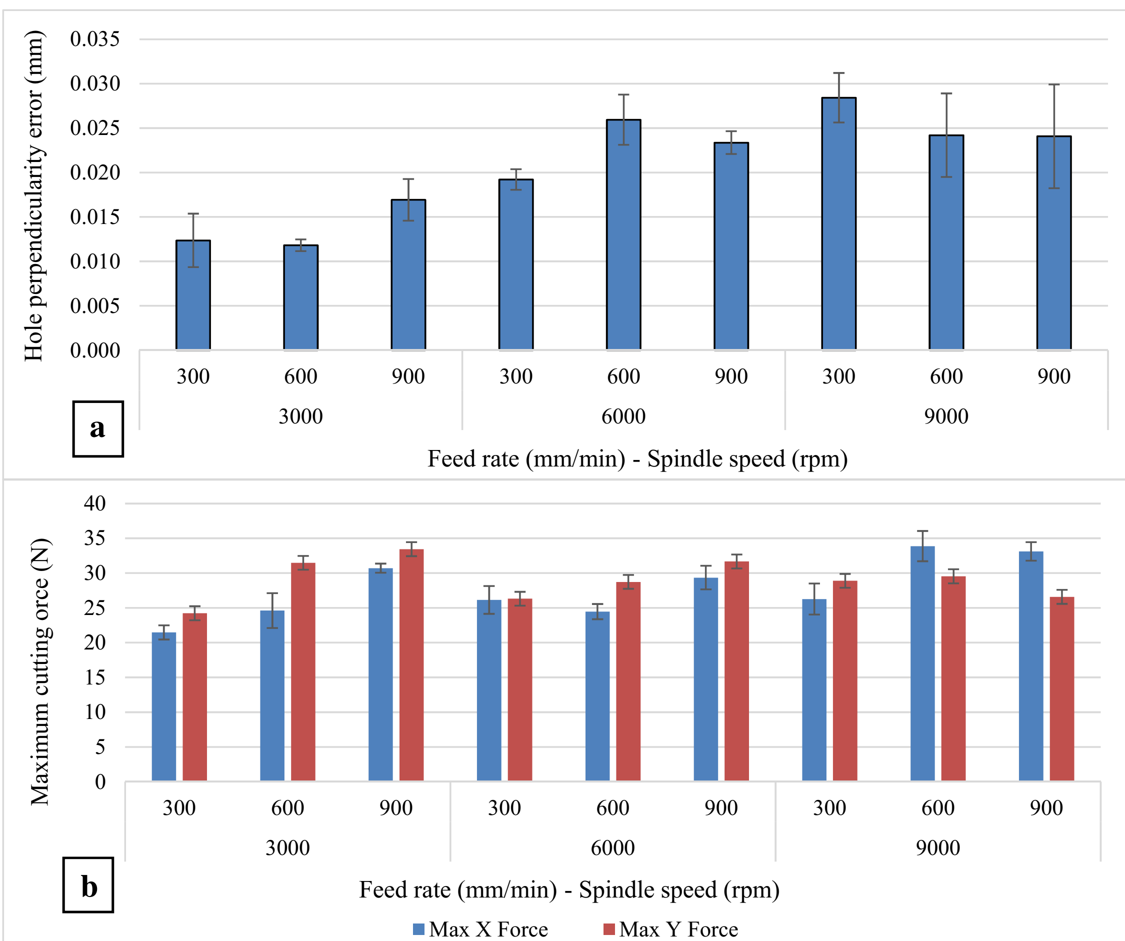

Fig. 9 GLARE 2B® laminate under cryogenic cooling conditions. **a** Hole perpendicularity error. **b** Cutting forces in the X and Y directions

Figure 10a shows the influence of cutting parameters on the average hole perpendicularity error at various flow rates and air pressures. The average hole perpendicularity error increased with the increase of feed rate and air pressure while it tended to decrease with the increase of spindle speed and coolant flow rate. The average hole perpendicularity error using MQL ranged between 0.004 and 0.015 mm. Increasing the coolant flow rate from 20 to 60 ml/h at a constant air pressure of 1 bar reduced hole perpendicularity error by 50%, and this was possibly due to the increased lubrication of the cutting tool. Increasing the air pressure from 1 to 3 bars at a constant coolant flow rate of 20 ml/h reduced hole perpendicularity error on average by 15%, which could be due to the improved chip evacuation from around the cutting. Minimum hole perpendicularity error occurred at low spindle speeds of $n = 3000$ rpm, low feed rates of $f = 300$ mm/min, and high flow rates of 60 ml/h regardless of the air pressure used which indicates that the coolant flow rate plays a significant role in reducing hole perpendicularity error. Increasing the air pressure from 1 to 3 bars helped reduce hole perpendicularity error but to a less extent than coolant rate. However, it was found that using moderate air pressure values of 2 bars seemed to reduce the error further. Applying higher flow rates and air pressure of cutting fluid in MQL to improve hole quality is only suitable when drilling at higher cutting speeds and feed rates, which indicates that using higher coolant flow rates can sometimes be unnecessary [78, 79]. In some cases, increasing air pressure increased hole perpendicularity error by 20%, which indicates that using excessive amounts of air pressure can have adverse effects on hole quality. This was possibly due to high air pressure reducing the performance of the lubricant due to lower amounts adhering to the cutting tool during the drilling process. However, it was observed that increasing the air pressure to 3 bars helped evacuate the chips from the cutting zone and reduced the likelihood of chips to curl around the cutting tool [9]. A high coolant flow rate of 60 ml/h and low to medium air pressure (1–2 bars) are recommended for minimal hole perpendicularity error. Figure 10b shows the cutting forces in X and Y directions under different cutting conditions. The results of cutting forces did not show any correlation with hole perpendicularity error which indicates that the impact of air pressure and coolant flow rate were more significant than the cutting forces. Cutting force data ranged between 15.5–28 N and forces were minimal when drilling at spindle speed of 6000 rpm, feed rate of 600 mm/min, and coolant flow rate of 40 ml/h and air pressure of 2 bars. This also corresponded to one of the lowest hole perpendicularity errors.

Figure 11a shows a comparison of hole perpendicularity error in GLARE® 2B laminates under dry, cryogenic, and MQL cooling conditions. The results of GLARE® drilling trials identified that the use of cryogenic liquid nitrogen cooling have an adverse impact on hole perpendicularity error. The hole perpendicularity error was significantly higher when applying LN2, while it increased when using MQL to a lower extent compared to dry drilling. Using MQL and LN2 coolants increased hole

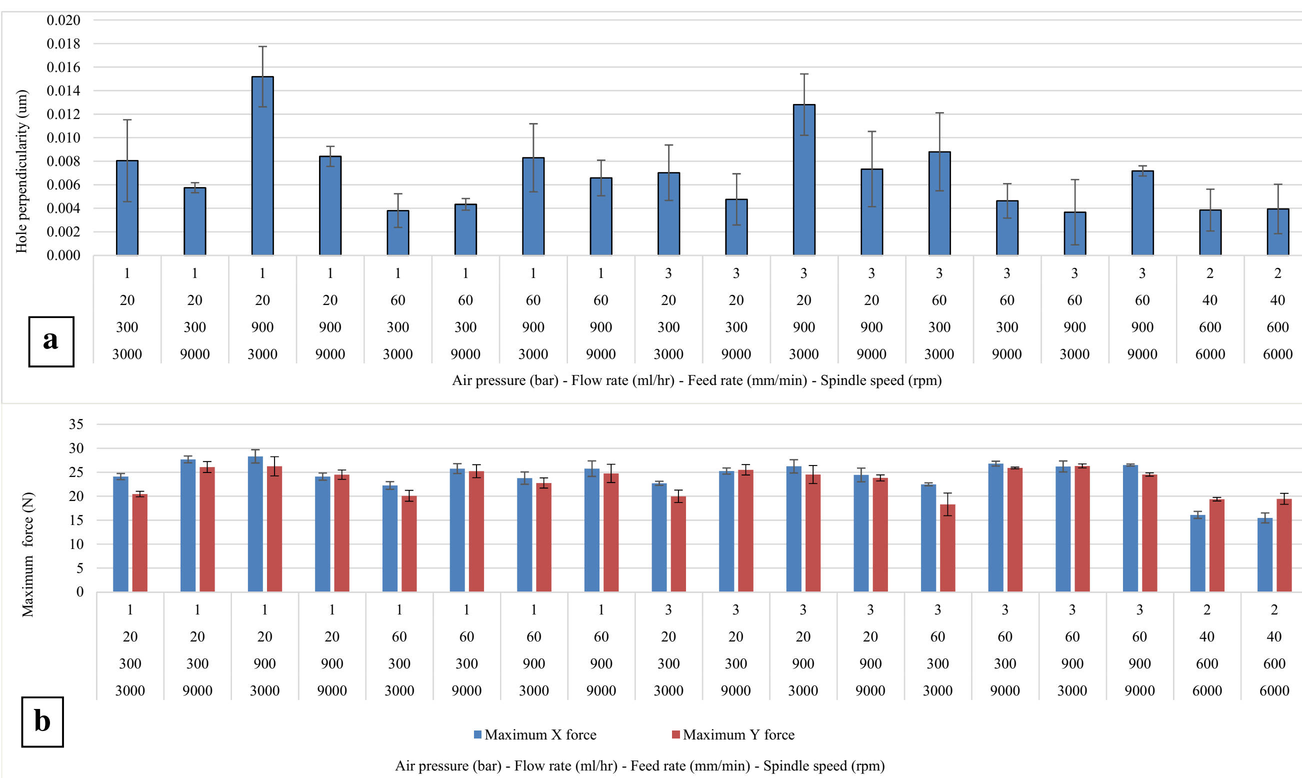

Fig. 10 **a**, **b** Hole perpendicularity error in GLARE 2B® laminate under MQL conditions

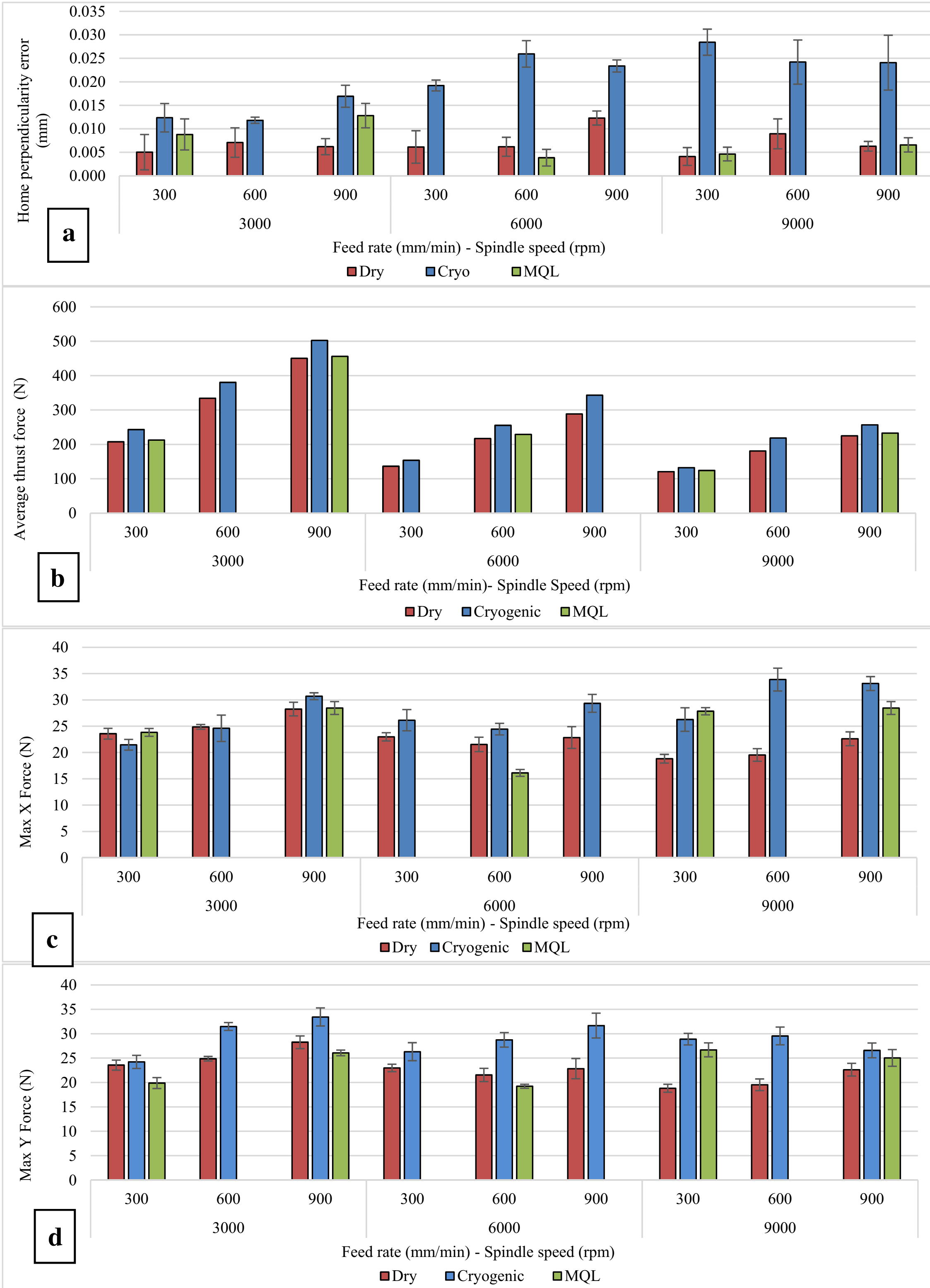

Fig. 11 The effect of coolant on **a** hole perpendicularity error, **b** average thrust force (F_z) [9, 59], **c** average maximum force in X direction (F_x), and **d** average maximum force in Y direction (F_y)

perpendicularity error compared to dry conditions by up to 116 and 700% receptively. It was also observed that the cutting forces in the X and Y directions were higher when using LN2 coolant as it can be noted from Fig. 11c, d. The impact of LN2 was greater than MQL, especially when drilling at high spindle speeds of 9000 rpm. This could be attributed to the sub-zero temperatures of the cryogenic cooling, which reduces the relaxation of the laminate during the machining process leading to distortion in the hole shape. Applying liquid nitrogen during machining reduces the amount of heat retained in the workpiece and preventing expansion in its constituents which could have adversely influenced hole perpendicularity error. This could be due to the change in the amount of plastic deformation—represented by the ductility and elongation of the material [80]. Additionally, hole perpendicularity can be influenced by the mechanical properties of the workpiece, such as its yield and ultimate strength which are influenced by the changes in the workpiece temperature during the machining process and the presence or absence of coolants [81]. Giasin et al. [8] previously reported that holes drilled in GLARE® laminates tended to be oversized when applying liquid nitrogen and MQL externally due to the reduced relaxation of the laminate during the machining process which distorts the hole walls through its thickness. Moreover, the limited access of the external MQL lubricant and cryogenic coolant supplied to some portion of the tool-chip interface at the start of the drilling process may have further increased the difference in thermal distortion effect at the upper and lower regions of the hole. This could be due to excessive coolant causing the drill to slide or aquaplane in the hole vicinity due to the formation of a lubricant layer between the circumference of the cutting tool and the workpiece surface [9], leading to difficulty in chip evacuation. Nandi et al. [65] previously stated that large amounts of coolant flow rate can sometimes deteriorate the surface finish when machining aluminum alloy AA1050 at high cutting speeds which could have also had an impact on hole perpendicularity [9, 65].

4 Conclusions

The machinability of GLARE® laminates was investigated through twist drilling process to evaluate hole perpendicularity error using a CMM machine. The aim is to evaluate the impact of cutting parameters (spindle speed and feed rate), cooling technologies namely cryogenic liquid nitrogen and minimum quantity lubrication cooling, fiber orientation, and depth of cut on hole perpendicularity error in GLARE® 2B and GLARE® 3 fiber metal laminates. The application of cryogenic and MQL coolants has been previously tested on other metals and composite materials, but never been applied and compared against each other in a single study for hole perpendicularity error on fiber metal laminates in the open literature. The application of these coolant is a trending issues and is still new to aerospace applications, while limited research have been carried out on the machinability of GLARE laminates. The research aims to investigate and build literature for the subject area and provide contribution to knowledge of the field of modern and environmentally friendly cooling technologies for future researchers. From the analysis of the experimental results, the following can be concluded:

- Drilling parameters (spindle speed and feed rate) have an impact on hole perpendicularity error. The spindle speed has greater effect on hole perpendicularity error and varied depending on the level of the feed rate and thickness of the laminate.
- Hole perpendicularity error is likely to be higher in thinner laminates due to increased bending of the workpiece and lack of support plate.
- Hole perpendicularity error was higher when drilling at spindle speeds of $n = 3000$ and 6000 rpm in GLARE® laminates in which fiber layers are orientated in the same direction (i.e., GLARE® 2B) than in cross ply GLARE® laminates with different fiber orientations.
- Previous studies reported that the drilling temperature depends on the fiber orientation which is higher for laminates with 90° fiber orientation than with 0° due to higher failure stresses [70, 71]. The rise in workpiece temperature increases the thermal distortions in the laminate and hole perpendicularity error.
- Under dry drilling, hole perpendicularity error was minimal at spindle speeds of $n = 3000$ rpm and feed rate of $f = 900$ mm/min for all tested GLARE® grades. Hole perpendicularity error was maximal when drilling at spindle speeds of $n = 3000$ rpm and feed rate of $f = 600$ and 900 mm/min.
- Using MQL and LN2 coolants increased hole perpendicularity error compared to dry conditions by up to 116 and 700% respectively. Applying LN2 significantly increased hole perpendicularity error and generated higher cutting forces on the hole walls in the X, Y, and Z directions compared to dry and MQL conditions.
- Under cryogenic drilling, hole perpendicularity error was minimal at spindle speeds of $n = 3000$ rpm and feed rate of $f = 300$ and 600 mm/min. Hole perpendicularity error was maximal when drilling at spindle speeds of $n = 9000$ rpm and feed rate of $f = 300$ mm/min.
- Under MQL drilling, hole perpendicularity error was minimal at spindle speeds of $n = 3000$ rpm, feed rate of $f = 900$ mm/min, coolant flow rate of 60 ml/h, and air pressure of 3 bars. Hole perpendicularity error was maximal when drilling at spindle speeds of $n = 3000$ rpm, feed rate of $f = 900$ mm/min, coolant flow rate of 20 ml/h, and air pressure of 1 bar.
- Limitations: the repeatability of hole perpendicularity error data was low, which indicates that other factors might have influenced the results which requires further investigation in future work. Other parameters include but not limited to the impact of the support plate and location of drilled hole on the workpiece.

Acknowledgments The author would like to thank the Advanced Manufacturing Research Centre (AMRC) at The University of Sheffield for the permission to use their facilities in this research project. The author would also like to thank Dr. Peter J. Kortbeek from the Fibre-Metal Laminate Centre of Competence (FMLC) and Professor Jose Sinke from DELFT University for their technical support on machining GLARE® and material supply. Special thanks to Mr. Jacob Hawxwell and Sandvik Coromant for the assistance with hole perpendicularity measurements.

Compliance with ethical standards

Conflict of interest The author declares no conflicts of interest.

References

1. Roebroeks GHJJ (1994) Fibre-metal laminates. Int J Fatigue 16(1): 33–42
2. Vlot A. *Glare: history of the development of a new aircraft material*. 2001: Springer Science & Business Media
3. Vlot A and Gunnink JW (2001) *Fibre metal laminates: an introduction*. Springer
4. Vlot A, Vogelesang L, De Vries T (1999) Towards application of fibre metal laminates in large aircraft. Aircr Eng Aerosp Technol 71(6):558–570
5. Sinmazçelik T et al (2011) A review: fibre metal laminates, background, bonding types and applied test methods. Mater Des 32(7): 3671–3685
6. Njuguna J (2016) *Lightweight composite structures in transport: design, manufacturing, analysis and performance*. Woodhead publishing
7. Giasin K, Ayvar-Soberanis S (2017) An investigation of burrs, chip formation, hole size, circularity and delamination during drilling operation of GLARE using ANOVA. Compos Struct 159:745–760
8. Giasin K, Ayvar-Soberanis S, Hodzic A (2016) The effects of minimum quantity lubrication and cryogenic liquid nitrogen cooling on drilled hole quality in GLARE fibre metal laminates. Mater Des 89: 996–1006
9. Giasin K, Ayvar-Soberanis S, Hodzic A (2016) Evaluation of cryogenic cooling and minimum quantity lubrication effects on machining GLARE laminates using design of experiments. J Clean Prod 135:533–548
10. Giasin K et al (2016) *3D finite element modelling of cutting forces in drilling fibre metal laminates and experimental hole quality analysis*. Appl Compos Mater:1–25
11. Giasin K, Ayvar-Soberanis S (2016) Evaluation of workpiece temperature during drilling of GLARE fiber metal laminates using infrared techniques: effect of cutting parameters, fiber orientation and spray mist application. Materials 9(8):622
12. Giasin K, Ayvar-Soberanis S, Hodzic A (2015) An experimental study on drilling of unidirectional GLARE fibre metal laminates. Compos Struct 133:794–808
13. Pawar OA et al (2015) Analysis of hole quality in drilling GLARE fiber metal laminates. Compos Struct 123:350–365
14. Tyczynski P, Lemanczyk J, Ostrowski R (2014) Drilling of CFRP, GFRP, glare type composites. Aircr Eng Aerosp Technol 86(4): 312–322
15. Paul S, Hoogstrate A, Van Praag R (2002) Abrasive water jet machining of glass fibre metal laminates. Proc Inst Mech Eng B J Eng Manuf 216(11):1459–1469
16. Praag RV, *Hand drilling fiber metal laminates, guideline for successful hand drilling*. Fiber metal laminates, Handbook of workshop properties, Delft University of Science & Technology, Structures & Materials Laboratory. 1996, Delft University of Science & Technology. 9
17. Praag RV, *Milling fiber metal laminate, tool wear tests, edge quality and justification of WP 3-200 to WP 3-250*. Fiber metal laminates, Handbook of workshop properties, Delft University of Science & Technology, Structures & Materials Laboratory. 1996, Delft University of Science & Technology. 19
18. van Praag R and Sinke J, (1994) *Manufacturing fibre-metal laminates: part 2: the forming properties*, Delft Univ Technol
19. Sinke J (2003) Manufacturing of GLARE parts and structures. Appl Compos Mater 10(4–5):293–305
20. Beumler T, *Flying GLARE: a contribution to aircraft certification issues in strength properties in non-damaged and fatigue damaged GLARE structures*. 2004: Delft University Press
21. Kim D, Ramulu M, Pedersen W (2005) Machinability of titanium/graphite hybrid composites in drilling. Trans NAMRI/SME 33: 445–452
22. Kim D, Ramulu M (2007) Study on the drilling of titanium/graphite hybrid composites. J Eng Mater Technol 129(3):390–396
23. Kim GW, Lee KY (2005) Critical thrust force at propagation of delamination zone due to drilling of FRP/metallic strips. Compos Struct 69(2):137–141
24. Sánchez Carrilero, M., et al. *Dry drilling of fiber metal laminates CF/AA2024. A preliminary study*. In *Materials science forum*. 2006. Trans Tech Publ
25. Pawar OA et al (2015) Analysis of hole quality in drilling GLARE fiber metal laminates. Compos Struct
26. Senthilkumar, B.M.A., *Mechanical and machinability characteristics of fiber metal laminates*. 2016: LAP Lambert Academic Publishing 60
27. Rezende BA et al (2016) Investigation on the effect of drill geometry and pilot holes on thrust force and burr height when drilling an aluminium/PE sandwich material. Materials 9(9):774
28. Welschen R, et al. *High pressure abrasive water jet machining of metal polymer laminates*. In *Proceedings of 17th All India Manufacturing Technology: Design and Research Conference*. 1997. Allied Publishers
29. Ramulu M, et al. (2015) *Abrasive waterjet machining effects on kerf quality in thin fiber metal laminate*, in 2015 *WJTA-IMCA Conference and Expo*, WJTA®-IMCA®: New Orleans, Louisiana
30. Ramulu M et al (2016) Experimental investigation of abrasive waterjet machining of titanium graphite laminates. Int J Autom Technol 10:392–400
31. Coesel JFW (1994) *Drilling of fibre-metal laminates*, in *Faculty of Aerospace Engineering*. Delft University of Technology. p. 63
32. GD&T. *Perpindicularity*. 2017 [cited 2017 21/02/2017]; Available from: http://www.gdandtbasics.com/perpendicularity/
33. Bickford J (1998) *Handbook of bolts and bolted joints*. CRC Press
34. Yuan P et al (2016) The attitude adjustment algorithm in drilling end-effector for aviation. Adv Mech Eng 8(1):1687814016629348
35. Liu J et al (2007) The effect of holes quality on fatigue life of open hole. Mater Sci Eng A 467(1):8–14
36. Yao S (2005) Evaluation of TiN/AlN nano-multilayer coatings on drills used for micro-drilling. Surf Coat Technol 197(2):351–357
37. Patel J, A.I., Patel D, Gandhi D, Patel N, Patel M (2014) *A review article on effect of cutting parameter on drilling operation for perpendicularity*. IOSR J Mech Civil Eng (IOSR-JMCE), 11(6)

38. Patel BP, P.M.G, Patel VJ, *Experimental studies on perpendicularity of drilling operation using DOE.* Int J Adv Eng Res Dev (IJAERD), 2014. 1(3)
39. Rysava Z et al (2016) Micro-drilling and threading of the Ti6Al4V titanium alloy produced through additive manufacturing. Procedia CIRP 46:583–586
40. Haan D et al (1997) An experimental study of cutting fluid effects in drilling. J Mater Process Technol 71(2):305–313
41. Sheth S, George P (2016) Experimental investigation, prediction and optimization of cylindricity and perpendicularity during drilling of WCB material using grey relational analysis. Precis Eng 45:33–43
42. Ahmed LS, Govindaraju N, Pradeep Kumar M (2016) Experimental investigations on cryogenic cooling in the drilling of titanium alloy. Mater Manuf Process 31(5):603–607
43. Govindaraju N, Shakeel AL, and Pradeepkumar M (2014) *Experimental investigations on cryogenic cooling in drilling of aluminium alloy.* In *Applied mechanics and materials*. Trans Tech Publ
44. Nair A, Kumanan S (2017) Multi-performance optimization of abrasive water jet machining of Inconel 617 using WPCA. Mater Manuf Process 32(6):693–699
45. Dhanabalan S, Sivakumar K, Sathiya Narayanan C (2014) Analysis of form tolerances in electrical discharge machining process for Inconel 718 and 625. Mater Manuf Process 29(3):253–259
46. Herghelegiu E, et al. (2017) *Considerations on material thickness influence on the AWJ processing quality of an aluminium alloy.* In *MATEC Web of Conferences*. EDP Sciences
47. Xueshu L et al (2017) Effects of hole-perpendicularity error on joint stiffness of single-lap double-bolt composite joints. Eng Trans
48. Akanksha P (2014) *Investigation of cutting parameters during drilling of Mildsteel in context of cylindricity and perpendicularity*, in *Engineering*, BVM Engineering College
49. Sheth S, et al. (2014) *Study and investigate effect of cutting parameters in drilling on cylindricity and perpendicularity.* In *Proceedings of the fourth national conference on recent advances in manufacturing (RAM-2014), SVNIT, Surat*
50. Manikandan N, Kumanan S, Sathiyanarayanan C (2017) Multiple performance optimization of electrochemical drilling of Inconel 625 using Taguchi based grey relational analysis. Eng Sci Technol, Int J 20(2):662–671
51. Selvarajan L, Narayanan CS, JeyaPaul R (2016) Optimization of EDM parameters on machining Si3N4–TiN composite for improving circularity, cylindricity, and perpendicularity. Mater Manuf Process 31(4):405–412
52. Selvarajan L, Sathiya Narayanan C, Jeyapaul R (2015) Optimization of process parameters to improve form and orientation tolerances in EDM of MoSi2-SiC composites. Mater Manuf Process 30(8):954–960
53. Kabakli E, Bayramoglu M, Geren N (2014) Evaluation of the surface roughness and geometric accuracies in a drilling process using the Taguchi analysis. Mater Technol 48(1):91–98
54. Alderliesten RC (2005) *Fatigue crack propagation and delamination growth in Glare*. DUP Science
55. De Vries TJ (2001) *Blunt and sharp notch behaviour of GLARE laminates*. TU Delft, Delft University of Technology
56. Mohit G, et al. (2011) *Predicting bearing strength of fiber metal laminates via progressive failure analysis*, in *52nd AIAA/ASME/ASCE/AHS/ASC Structures, Structural Dynamics and Materials Conference*, Am Inst Aeronaut Astronaut
57. Yaghoubi AS and Liaw B (2013) *Damage assessments of ballistic impact behaviors of GLARE 5 (3/2) beams with various stacking sequences*, in *Dynamic behavior of materials, Volume 1*, Springer. p. 503–512
58. Hagenbeek M (2005) *Characterisation of fibre metal laminates under thermomechanical loadings*. TU Delft, Delft University of Technology
59. Giasin K (2017) *Machining fibre metal laminates and Al2024-T3 aluminium alloy*, University of Sheffield
60. Kelly J, Cotterell M (2002) Minimal lubrication machining of aluminium alloys. J Mater Process Technol 120(1):327–334
61. Braga DU et al (2003) Minimum lubrication in Al-Si drilling. J Braz Soc Mech Sci Eng 25:63–68
62. Braga DU et al (2002) Using a minimum quantity of lubricant (MQL) and a diamond coated tool in the drilling of aluminum–silicon alloys. J Mater Process Technol 122(1):127–138
63. Sreejith PS (2008) Machining of 6061 aluminium alloy with MQL, dry and flooded lubricant conditions. Mater Lett 62(2):276–278
64. Davim J et al (2006) Experimental studies on drilling of aluminium (AA1050) under dry, minimum quantity of lubricant, and flood-lubricated conditions. Proc Inst Mech Eng B J Eng Manuf 220(10):1605–1611
65. Nandi AK, Paulo Davim J (2009) A study of drilling performances with minimum quantity of lubricant using fuzzy logic rules. Mechatronics 19(2):218–232
66. Bhowmick S, Alpas AT (2008) Minimum quantity lubrication drilling of aluminium–silicon alloys in water using diamond-like carbon coated drills. Int J Mach Tools Manuf 48(12–13):1429–1443
67. Bhowmick S, Lukitsch MJ, Alpas AT (2010) Dry and minimum quantity lubrication drilling of cast magnesium alloy (AM60). Int J Mach Tools Manuf 50(5):444–457
68. Murthy KS, Rajendran IG (2012) Prediction and analysis of multiple quality characteristics in drilling under minimum quantity lubrication. Proc Inst Mech Eng B J Eng Manuf 226(6):1061–1070
69. Martin O (2015) *Metrology enabled tooling for the assembly of aero-structures*, University of Bath
70. Zitoune R et al (2005) Experiment–calculation comparison of the cutting conditions representative of the long fiber composite drilling phase. Compos Sci Technol 65(3):455–466
71. Ghafarizadeh S, Lebrun G, and Chatelain J.-F (2015) *Experimental investigation of the cutting temperature and surface quality during milling of unidirectional carbon fiber reinforced plastic.* J Compos Mater: p. 0021998315587131
72. Strong AB (2008) *Fundamentals of composites manufacturing: materials, methods and applications*. Society of Manufacturing Engineers
73. Chung DDL (2010) *Composite materials: science and applications*. Springer London
74. Park C and Mcmanus HL (1994) *Thermally induced damage in composite space structure: predictive methodology and experimental correlation*. p. 26
75. Giasin K, Ayvar-Soberanis S (2017) Microstructural investigation of drilling induced damage in fibre metal laminates constituents. Compos A: Appl Sci Manuf 97:166–178
76. Zitoune R, Krishnaraj V, Collombet F (2010) Study of drilling of composite material and aluminium stack. Compos Struct 92(5): 1246–1255
77. Isbilir O, Ghassemieh E (2013) Comparative study of tool life and hole quality in drilling of cfrp/titanium stack using coated carbide drill. Mach Sci Technol 17(3):380–409
78. Dixit US, Sarma D, and Davim JP (2012) *Environmentally friendly machining*. Springer Science & Business Media
79. Mendes O et al (2006) The performance of cutting fluids when machining aluminium alloys. Ind Lubr Tribol 58(5):260–268
80. Köklü U (2012) Influence of the process parameters and the mechanical properties of aluminum alloys on the burr height and the surface roughness in dry drilling. Materiali in tehnologije 46(2): 103–108
81. Lauderbaugh LK (2009) Analysis of the effects of process parameters on exit burrs in drilling using a combined simulation and experimental approach. J Mater Process Technol 209(4):1909–1919